Health Scope. 2019 November; 8(4):e88454. doi: 10.5812/jhealthscope.88454.
Published online 2019 October 29. **Research Article**

Removal of Malathion by Sodium Alginate/Biosilicate/Magnetite Nanocomposite as a Novel Adsorbent: Kinetics, Isotherms, and Thermodynamic Study

Mehdi Hosseini [1, *], Hossein Kamani [2], Ali Esrafili [1], Mojtaba Yegane Badi [1] and Mitra Gholami [1, **]

[1]Department of Environmental Health Engineering, Research Center for Environmental Health Technology, School of Public Health, Iran University of Medical Sciences, Tehran, Iran
[2]Department of Environmental Health, Health Promotion Research Center, Zahedan University of Medical Sciences, Zahedan, Iran

[*]*Corresponding author*: Department of Environmental Health Engineering, Research Center for Environmental Health Technology, School of Public Health, Iran University of Medical Sciences, Tehran, Iran. Email: hosene_m@yahoo.com
[**]*Corresponding author*: Department of Environmental Health Engineering, Research Center for Environmental Health Technology, School of Public Health, Iran University of Medical Sciences, Tehran, Iran. Email: gholamim@iums.ac.ir

Received 2018 December 30; **Revised** 2019 August 01; **Accepted** 2019 February 18.

Abstract

Background: Organophosphorus pesticides are one of the widely consumed poisons in agriculture. The consumption of drinking water, which contains an excessive amount of poison, therefore, contributes to adverse health and hygiene outcomes in humans.
Methods: In this study, a new sodium alginate/biosilicate/magnetite (SABM) nanocomposite made by the precipitation method was used to remove Malathion from aqueous solutions. The properties of MBSA were analyzed using XRD, SEM, EDX, and FTIR techniques. The possible impact of several parameters such as contact time, pH, initial Malathion concentration, temperature, and MBSA dosage on the adsorption process were investigated. The equilibrium isotherm and kinetic models were employed to evaluate the fitness of the experimental data.
Results: The highest removal (94.82%) of MBSA was obtained at an optimum pH of 7, the contact time of 120 minutes, the adsorbent dosage of 4 g/L, Malathion concentration of 10 mg/L, and temperature of 318°K. The adsorption process followed the Freundlich isotherm model (R^2 = 0.999), which implied that the adsorption process of Malathion molecules onto MBSA might be mainly a multi-molecular layer.
Conclusions: The results of this study showed that MBSA had a good removal efficiency, lower cost of processing, and as well as not producing substances harmful to the environment, which make it a promising adsorbent to remove Malathion from aqueous environments.

Keywords: Malathion, Removal, Sodium Alginate, Biosilicate, Nanocomposite

1. Background

In the last few decades, pesticide contamination of water resources has emerged as a worldwide ecological concern. These compounds also have been detected in surface water and in bed sediments that its documents are available. Their concentration in aqueous sources is very variable and much higher concentrations of them have been reported in the effluents of farmlands.

Organophosphorus pesticides are the most common pesticides in the world. Unfortunately, their uncontrolled consumption in many parts of the world has contributed to their overabundance in the environment (1, 2). The pesticides used in agriculture can find a way into the surface water bodies through irrigation and precipitation which results in pollution of these waters (3). One of these pesticides is Malathion [(2dimethoxyphosphorothioyl) sulfanyl], which is a frequently used pesticide. The pesticides are widely used to increase the productivity of agricultural products as well as to control the diseases transmitted by arthropods (4). Organophosphorus pesticides such as Malathion are considered a serious threat to human health due to their effects on the cholinesterase activity and central nervous system disorder (5). Malathion may persist in water with a half-life of months or even years. The World Health Organization (WHO) has set the pesticide in drinking water at 0.1 $\mu g\ L^{-1}$ (6).

Malathion has a high solubility in water and its removal by conventional treatment processes such as sand filtration and coagulation is a really difficult process (7).

Results from the previous studies indicate that in order to eliminate these pesticides, various methods such as photocatalytic degradation (8), biological oxidation (9), advanced oxidation processes (AOPs) (10), and adsorption (11, 12) have been employed. Among these techniques, adsorption process is a desirable method to remove pesticides. The adsorption technique is known for its simplicity, reliability, safety, and low costs that is an economical and effective method, and also a friendly environmental process (13-15).

The silica compounds are a desirable adsorbent because of the ability of their surface functional groups to adsorb target pollutants (16, 17). Diatomite soil, also called biosilica, is a porous biodegradable silica stone containing 87.0% - 91.0% silicon dioxide. Because of high surface area and active-surface agents, the biosilica is a suitable adsorbent for adsorbing contaminants from water solution (18, 19). Among the various adsorbents, nanostructured adsorbents have attracted the attention of researchers as a result of their vast surface area and their very active surface sites rather than large adsorbents (20, 21). One of the well-known nanostructures is magnetite nanoparticles that have been used owing to its surface area, and its ability in combination with other adsorbents in the synthesis process of nanoparticles (22, 23). In addition, the main advantage of magnetite nanoparticles is to be easily separated from aqueous solutions by an external magnetic field. However, its adsorption capacity and selectivity are not satisfactory, and also has shown to have poor stability in acidic conditions (13). One of the great problems in the use of nano-sized adsorbents is the separation and recycling of the adsorbents. In order to achieve this objective is to fix the adsorbent material inside another material. Polymeric compounds such as chitosan and alginate are the most widely used materials and they are suitable for stabilizing nanoparticles. Among the various polymers, alginate is considered an important category of organic matter. Alginate has unique properties such as environmental compatibility, low cost and non-reactivity in the adsorbent composition (14, 24). However, using sodium alginate/biosilicate/magnetite (SABM) nanocomposite for removal of Malathion has not been reported in the literature.

2. Objectives

The purpose of this study was to determine the efficiency of SABM nanocomposite in the removal of Malathion from aqueous environments. The possible impact of several parameters such as contact time, pH, initial Malathion concentration, temperature, and adsorbent dosage on the sorption process were investigated. The Langmuir and Freundlich adsorption isotherm was used to evaluate the adsorption capacity of SABM.

3. Methods

3.1. Chemicals

In this study, sodium hydroxide (NaOH), hydrochloric acid (HCl), acetic acid (CH_3CO_2H), ferric chloride ($FeCl_3.6H_2O$), ferrous sulfate ($FeSO_4.7H_2O$), sodium triphosphate ($Na_5P_3O_{10}$), ammonia solution, and sodium alginate were from Merck and Diatomite was from Sigma Aldrich. Also, Malathion, 95.0% of active ingredient was purchased from Sigma Aldrich. To make solutions needed by the experiments, deionized water was used.

3.2. Preparation of Adsorbent

There are two main steps in preparation of the adsorbent used in this study. First, making magnetite nanoparticles. Second, preparing the nanocomposite of SABM. These two steps are explained in the following.

3.3. Preparation of Magnetite Nanoparticles

A chemical coprecipitation method was used to prepare the magnetite nanoparticles. In this method, $FeSO_4.7H_2O$ and $FeCl_3.6H_2$ were first dissolved in a 1:1 ratio with a concentration of 3.2 M in the deionized water. The mixture was stirred in the presence of nitrogen gas at 80°C for 30 minutes. Then the ammonia solution with a purity of 25.0% was added to the mixture to reach the pH 10, and again it was washed under nitrogen gas for 60 minutes. The resulted magnetite nanoparticles were separated from the solution using a magnet, and then it was washed several times with ethanol and deionized water. The washed nanoparticles were dried at 70°C for 24 hours (25).

3.4. Preparation of Sodium Alginate/Biosilicate/Magnetite Nanocomposite Adsorbent

To prepare the nanocomposite, first 1 g of sodium alginate was added to 100 mL of acetic acid solution (1 M) and mixed for 2 hours. Then 1g of biosilicate and 1g of magnetite were added to the solution, and that was stirred by a stirrer at a fixed speed. To remove all bubbles in the solution and to obtain a no-bubble mixture, the resulting mixture was placed under a stable situation for 10 hours. In the next, a 100 mL mixture of NaOH (15.0%) and ethanol (95.0%) with ratio of 4:1 was prepared, and then the mixed solution of sodium alginate/biosilicate/magnetite was added to the mixture using a droplet, and then the solution was stored for 24 hours to form granular particles.

Then the granular particles were washed with distilled water and dried at the ambient temperature to reach a constant weight. Finally, the dried mixture was chopped and then it was passed through a sieve to obtain the nanocomposite in a proper size (26). In the following, sodium alginate/biosilicate/magnetite nanocomposite adsorbent was signified by abbreviation of SABM adsorbent.

3.5. Characterization of SABM Adsorbent

A scanning electron microscope (SEM, Jeol ModelJsm-T330) with equipped an X-ray energy spectroscopy (EDX) under vacuum stable was used to determine the surface morphology and composition of the prepared SABM adsorbent. The crystal structure and purity of the SABM adsorbent particles in this work were characterized by X-ray diffraction (XRD) patterns, which were obtained on a Bruker D8 Advance X-ray diffractometer with Cu Kα radiation. The diffraction images were recorded at 40 mA and 40 kV in the 2θ range of 10° - 80°. Also, to recognize the SABM adsorbent functional groups involved in the adsorption process, it was used a Fourier transform infrared (FTIR) adsorption spectrophotometer (JASCO, FT/IR-6300Japan) using KBr disc method. The FTIR adsorption spectra were recorded in the range of 400 to 4000 cm^{-1}.

3.6. The pH at Point Zero Charge (pHzpc)

To determine pH at zero pH point (pH_{ZPC}) of the SABM adsorbent, the following steps were conducted. At first of all, a sufficient amount of 0.1 M $NaNO_3$ solution was spilled into 250 mL flacks and their pH was adjusted between 2 and 11 by either 1 M HCl or NaOH. The whole volume of the solution in each flask was reached to 100 mL by adding $NaNO_3$ solution of the same known concentration; meanwhile, the initial pH values of the solutions were accurately recorded. In the next step, 0.15 g of SABM adsorbent was added to each of the flasks and placed on a shaker at 200 rpm for 24 hours. Finally, the SABM adsorbent was separated from the suspensions, and then the pH values of the solution (final pH) were recorded. The pH_{ZPC} was obtained by plotting the initial pH values versus the final pH values (27).

3.7. Adsorption Experiments

This study was conducted in a batch system as a factor at the time. The effect of parameters, including contact time, initial pH values of the solution, SABM adsorbent dose, initial concentration of Malathion, and temperature of the solution was investigated on the adsorption of Malathion onto the SABM adsorbent. Also, adsorption kinetics and isotherms were studied.

The experiments were carried out in the following steps. In the first stage of experiments, a 100 mL suspension, including Malathion (5.0 mg L^{-1}) and SABM adsorbent (0.5, 1, 1, 2 and 2.5 g L^{-1}) were spilled into the 250 mL conical flasks and initial pH values were adjusted at 3, 5, 7, 9 and 11 using NaOH and HCl solution, and then it was placed on the thermoshaker at 200 rpm and 25°C, to shake for 120 minutes. The pH was measured with a pH meter (Aqua lytic (AL15)). To investigate Malathion concentration effect, the experiments were carried out at various concentrations (5, 25, 50 and 100 mgL^{-1}) at pH 7 and SABM adsorbent dose 2 gL^{-1} at 25°C. Finely, effect of temperature on the adsorption process was carried out at various temperatures of solution (25, 35 and 40°C) and pH 7, adsorbent dose 2 gL^{-1} and Malathion concentration 5 mgL^{-1}. The temperature was adjusted by incubator shaker.

3.8. Analysis

At the end of each experiment, a magnet was used to remove the SABM adsorbent from the suspension, (1.3 T), and then the residual of Malathion in the solution was measured with a UV-Vis spectrophotometer (DR 6000) at λ_{max} of 236 nm. The removal efficiency of the adsorption process was calculated using Equation 1.

$$Adsorption\ (\%) : \frac{C_0 - C_t}{C_0} \quad (1)$$

Where C_0 and C_t are initial and final concentrations of Malathion, respectively.

The adsorption capacity was also calculated using Equation 2.

$$q_t : \frac{(C_0 - C_t)\, V}{m} \quad (2)$$

Where C_0, C_t, V, and m, are initial concentration and the final concentration of Malathion, the volume of solution (L) and the mass of adsorbent particles (g), respectively.

4. Results and Discussions

4.1. Characterization of Adsorbent

The scanning electron micrographs of SABM, sodium alginate, biosilica, and magnetic are shown in Figure 1. As shown in Figure 1D, the porosity of the SABM adsorbents is much more than other adsorbents. Such porosity level enhances the capacity and efficiency of Malathion adsorption onto SABM adsorbents. The elemental analysis of the adsorbent composition of SABM is shown in Figure 2. As can be seen, sodium, oxygen, iron, silica and aluminum presence in adsorbent structure. Moreover, the results revealed that silica can prevent the oxidation of iron nanoparticles by acid, which has been used in the process of adsorbent

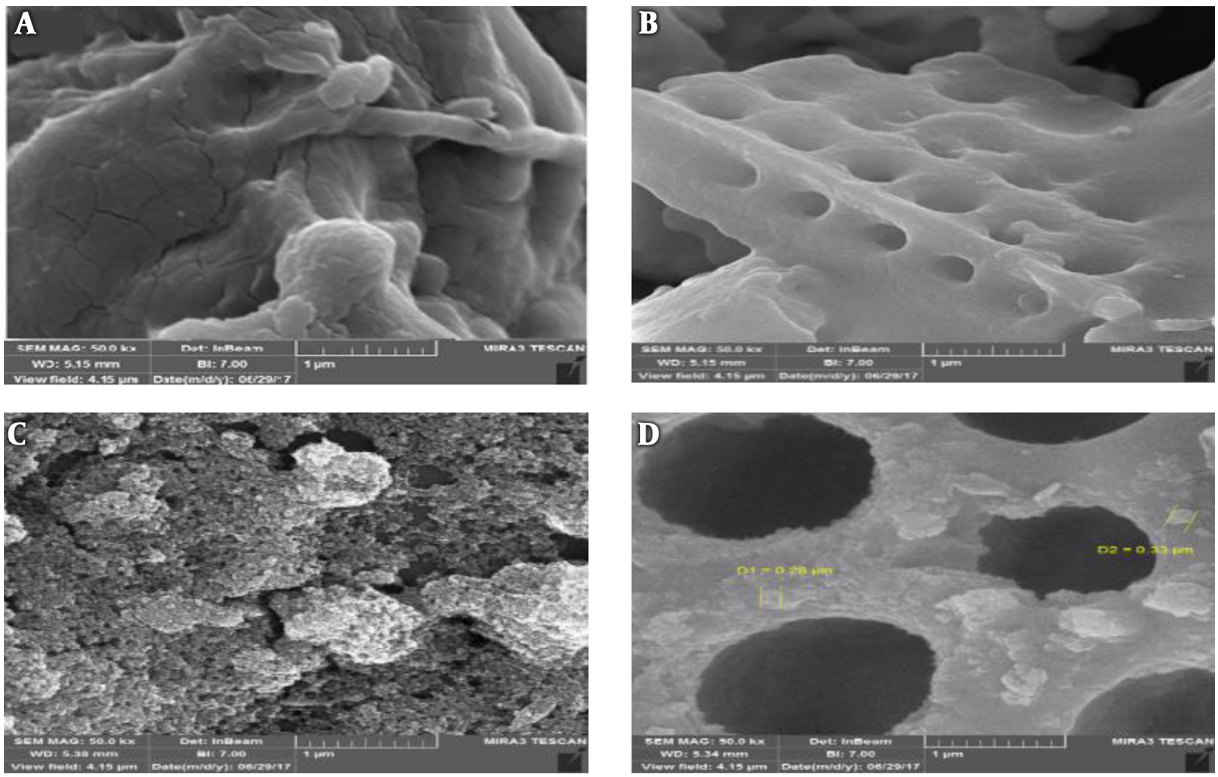

Figure 1. SEM of adsorbent particles, A, sodium alginate, B, biosilica, C, magnetic, and D, SABM is shown

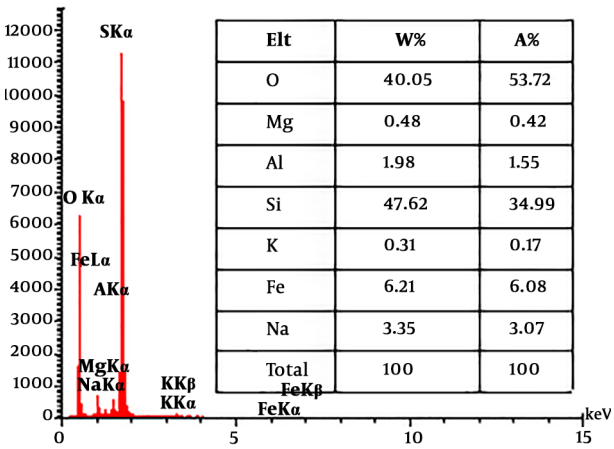

Elt	W%	A%
O	40.05	53.72
Mg	0.48	0.42
Al	1.98	1.55
Si	47.62	34.99
K	0.31	0.17
Fe	6.21	6.08
Na	3.35	3.07
Total	100	100

Figure 2. EDX analytical results of SABM are shown

synthesis. These findings point out the suitable composition of the materials applied to the synthesis of SABM.

The XRD pattern of SABM is shown in Figure 3. In the magnetite pattern, the deflected peaks at the 2θ of 30.6, 36.04, 43.6, 54.2, 57.6, and 63.25 which are related to the crystalline plates (220, 311, 400, 422, 511, and 440) and they agree with the Fe_3O_4 cubic phase JCPDS (card No. 19-0629) (22). Also, there are some peaks in the SABM pattern indicating the presence of Fe_3O_4 in the SABM compound. As can be seen in Figure 3, the peaks obtained for the biosilica are in accordance with the pure silica phase (JCPDS ICDD File Card # 00-001-0647), and are quite obvious in the SABM pattern. Moreover, as shown in Figure 3 the intensity of the peaks in the composite SABM is reduced to the Fe_3O_4 and biosilica which can be related to the combination of these two substances with alginate because alginate have amorphous nature and it affects the pattern of SABM (26). FTIR spectroscopy is a powerful, well-developed method to determine the structure and identification of chemical species. It is mainly used to identify organic compounds because of the complexity of their spectra (5). The FTIR spectroscopy is a powerful, well-developed method to determine the structure and identification of chemical species. It is mainly used to identify organic compounds because of the complexity of their spectra (28). The FTIR spectrum of sodium alginate, magnetite, biosilica and SABM (before and after the adsorption of Malathion onto

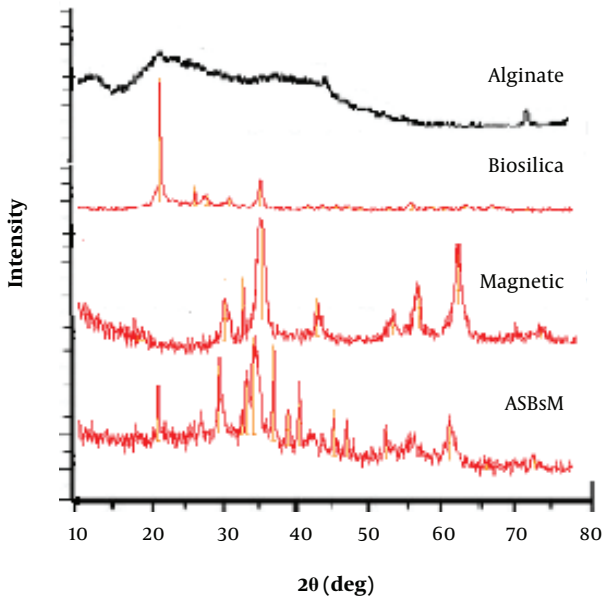

Figure 3. XRD results of SABM are shown

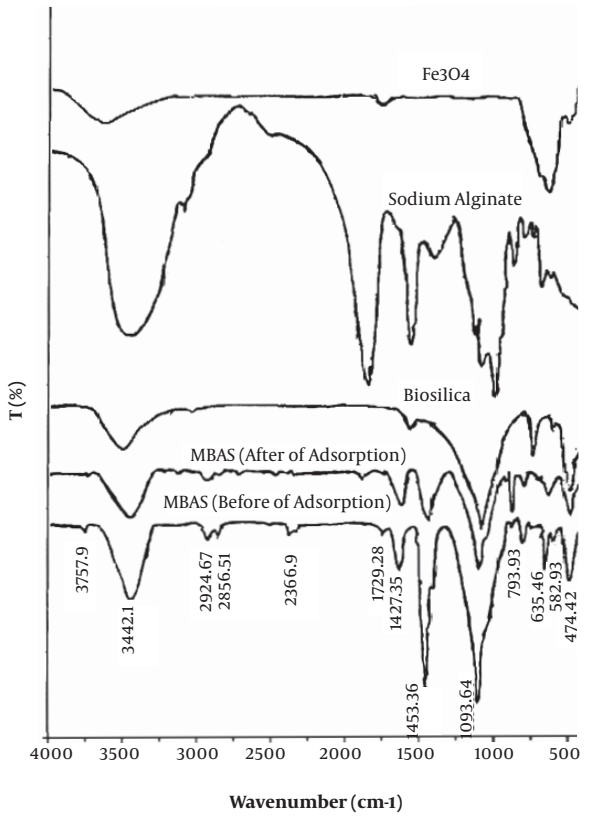

Figure 4. FTIR spectra of sodium alginate, magnetite, biosilica, and SABM are shown

the SABM) is depicted in Figure 4. It's shown that some obvious changes take place in the spectrum of SABM in comparison with the pristine sodium alginate spectrum and bare magnetite. Also, considering Figure 4, the bands 1626 and 1453 are carboxylic anions (COO-). Owing to the polysaccharide property of the alginate, the band 1093 (C-O-C asymmetric traction) is visible. The strong and broad-band 3442 is related to the stretching vibration of O-H groups (18). As known (Figure 4) in the magnetite spectrum, four major peaks are considerable. The 3450 band relates to the stretching vibration of O-H groups and the other three bands (635, 582 and 474) relate to the Fe-O vibrational bands (22). Comparison between the two spectra of the SABM adsorbent (before and after the adsorption of Malathion showed that the intensity of peaks at 3422, 2924, 2366, 627, 1453, 1093, 793, 627, and 454 was reduced after the adsorption of Malathion on the SABM, which indicated the impact of these functional groups on the adsorption process and confirmed that the magnetite nanoparticles were successfully coated with sodium alginate.

4.2. Effect of Contact Time

To investigate the adsorption behavior depended on time, the adsorption process was carried out at a determined statue for 4 hours. Figure 5 shows the result of the contact time effect on the adsorption process. As shown in Figure 5, the Malathion removal efficiency was increased immediately within 10 minutes (20.0%), then it was observed a stable pattern in the removal efficiency until 120 minutes, where the equilibrium was established and the removal efficiency was 92.1%.

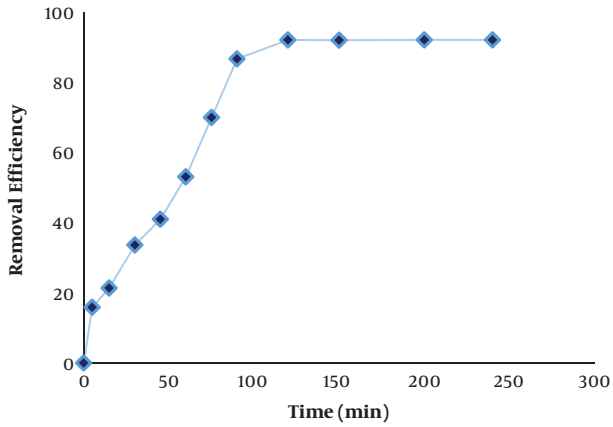

Figure 5. Effect of contact time is shown

4.3. Effect of pH

The effect of pH values on the removal of Malathion by the SABM adsorbent is shown in Figure 6A, where pH values were (3, 5, 7, 9, and 11), adsorbent dose was 1 g L^{-1}, concentration of Malathion was 5 mg L^{-1}, and temperature was 25°C at contact times 120 minutes. As can be seen, the highest removal efficiency of Malathion occurred at pH 7 and the lowest removal was at pH 11 (Figure 6). With an increase of pH from 3 to 7, the removal efficiency of Malathion has increased, but the removal efficiency has decreased with increasing pH from 7 to 9 and 11, respectively. In a previous study, a similar result has been reported by Kumar et al. (29) and by Zhang et al. (30) on the removal of Malathion by using both agricultural and commercial adsorbents. Concerning the effect of pH on the adsorption process, it is believed that determining pH_{ZPC} is important in the justification of the obtained results. Based on Figure 6B, pH_{ZPC} of SABM adsorbent was in 9.6. When the pH value is higher the pH_{ZPC}, the charge of adsorbent is negative and when it is lower the pH_{ZPC}, the charge of adsorbent is positive (15). Owing to the presence of electronegative centers (S and P) on the Malathion structure, and the SABM adsorbent pH_{ZPC} (9.6) (30), the Malathion can be adsorbed onto the SABM adsorbent at the acidic and natural pH best of alkaline pH values.

4.4. Effect of the Adsorbent Dose

Effect of various doses of adsorbent (0.5, 1, 1.5, 2, and 2.5 g L^{-1}) in the Malathion adsorption onto the SABM adsorbent was shown in Figure 7A, where pH and concentration of Malathion were 7 and 5 mg L^{-1} and temperature was 25°C, respectively. As can be seen in Figure 7A, an increase in the SABM dose enhanced removal efficiency where the lowest and highest removal efficiency are in the SABM dose 0.5 and 2.5 g L^{-1}, respectively. In a past study, a similar result has been observed by (7, 29). It is obvious that with increasing mass of adsorbent, the active site to adsorb pollutant increased that led to an increase in the removal efficiency of Malathion onto the SABM adsorbent (27).

4.5. Effect of the Initial Concentration of Malathion

One of the most important and influential factors in the adsorption process is the initial concentration of pollutants. Therefore, the effect of the initial different concentrations (5, 25, 50, and 100 mgL^{-1}) of Malathion on the removal efficiency of the adsorption process was investigated, as pH and SABM dose were 7 and 2 g L^{-1} and temperature was 25°C, respectively, and the results were presented as Figure 7B. As can be seen in Figure 7B, when the Malathion initial concentration increased from 5 to 100 mg L^{-1}, removal efficiency of Malathion decreased from 92.1% to 45.5%. This result agreed with the previous study by Kumar et al. (29) by which the Malathion was adsorbed onto the both agricultural and synthetic adsorbents. This phenomenon occurred because of a constant dose of SABM in contrast to the increased concentration of Malathion that reduced removal efficiency of the adsorption process. With an increase in the Malathion concentration, the active sites and surface area of the SABM become inadequate (29).

4.6. The Effect of Temperature

The results of the temperature effects on the removal efficiency of Malathion by SABM adsorbent are shown in Figure 8A. As can be seen, an increase in the temperature led to an increase in the adsorption of Malathion Figure 8A. The highest removal efficiency of Malathion is at 45°C (85.0%) and the lowest of it is at 25°C (92.0%). Hence, it can be explained by this fact that the adsorption process was endothermic in nature. This phenomenon can occur due to an increase in the displacement from the solubility phase of the molecules and their penetration within the pores of the SABM adsorbent (31, 32).

4.7. Isotherm of Adsorption

To investigate the distribution of adsorbated molecules onto the adsorbent in equilibrium, the adsorption isotherm was employed. In this study, the relationship between the concentration of Malathion in solution and its adsorbed amount were determined by the Freundlich and Langmuir isotherms (15, 31).

The Langmuir isotherm model declares that the distribution of solute molecules onto the adsorbent surface has a monolayer pattern. As a solute molecule attaches to the active site placed on the adsorbent, no further adsorption can occur at that site (32, 33). The linear form of Langmuir isotherm model is expressed via Equation 3:

$$\frac{C_e}{q_e} = \frac{1}{K_a q_m} + \frac{C_e}{q_m} \quad (3)$$

Separation factor (R_L), which is a dimensionless parameter, is defined via Equation 4:

$$R_L = \frac{1}{1 + K_a C_0} \quad (4)$$

Where Langmuir constants (C_e, q_e, q_m, and K_a) are attributed to the equilibrium concentration of Malathionin solution (mg L^{-1}), amount of adsorbed Malathion (mg g^{-1}), maximum monolayer adsorption capacity (mg L^{-1}) and energy of adsorption (L mg^{-1}), respectively, are calculated from plat of C_e/q_e versus C_e (15, 34). In Table 1, the results of Langmuir constants in modeling SABM adsorbent were presented calculated. With plotting C_e/q_e versus C_e for

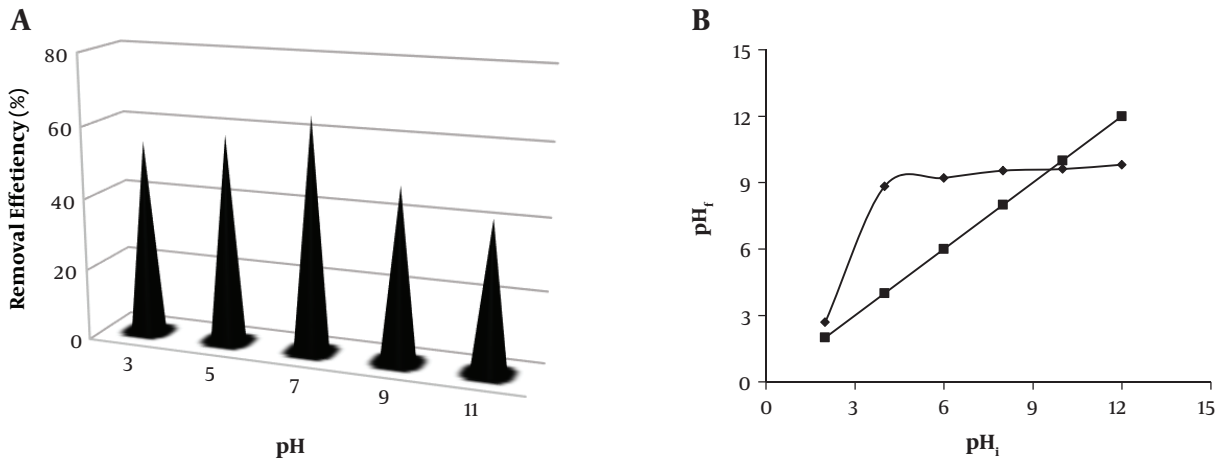

Figure 6. Effects of pH on the removal of Malathion from the SABM (A) and pH_{ZPC} (B) are shown

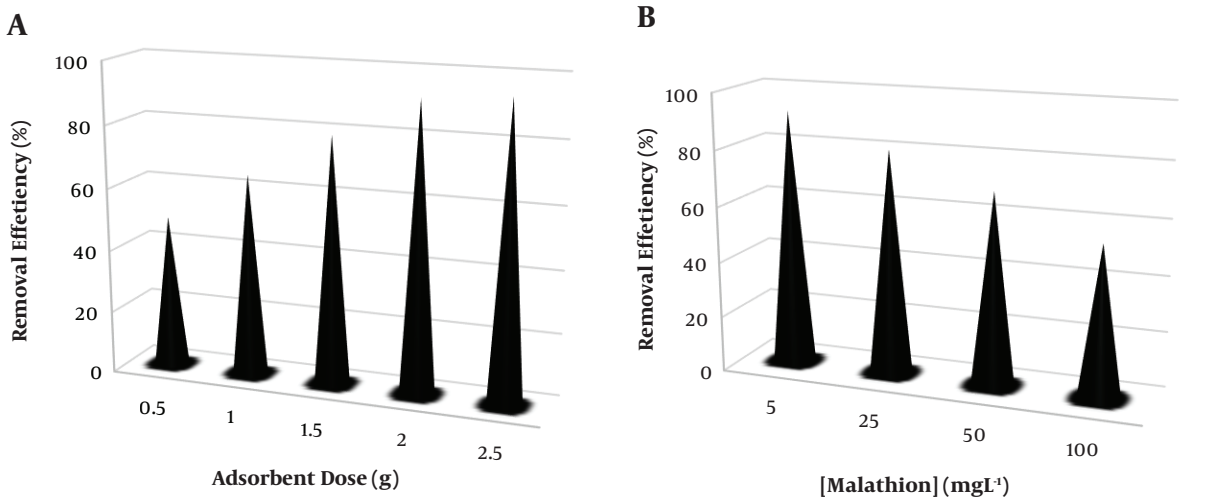

Figure 7. Effects of absorbent dose (A) and initial concentration of Malathion (B) on the removal of Malathion from the SABM are shown

Langmuir isotherm model, not provided here, it appears that this isotherm model has a poor coefficient of determination (R^2 = 0.852) in fit of the adsorption process. As can be seen in Table 1, Langmuir constants q_m, R_L, and K_a are 36.76 (mg g^{-1}), 0.011 and 17.24 (L mg^{-1}), respectively. This q_m for SABM adsorbent was higher than what was reported in the previous study by Darvishi Cheshmeh Soltani et al. (26) conducted in desorption of a textile dye using biosilica/chitosan nanocomposite. Also, a study of Malathion removal by agricultural and commercial adsorbents that was carried out by Kumar et al. (29), showed a q_m = 25 (mg g^{-1}) which is lower than what reported in this study. The comparison of q_m of SABM for Malathion removal with the other similar nanomaterial sorbents under similar experimental conditions is shown in Table 2. In this study, R_L (dimensionless parameter) that indicates relative volatility in vapor-liquid equilibrium with a range between 0 and 1 for a favorable equilibrium (15), is at the favorable range. Therefore, it can be concluded that adsorption of Malathion onto the SABM adsorbent had a good favorable equilibrium.

Freundlich isotherm model was used to determine the multilayer adsorption of adsorbate on the adsorbent surface. It also assumes that adsorption occurs on heterogeneous surfaces and can be expressed via Equation 5. (27).

$$log\ q_e = logK_f + \frac{1}{n}\,(logC_e) \quad (5)$$

Where Freundlich isotherm constants (K_f and n) are

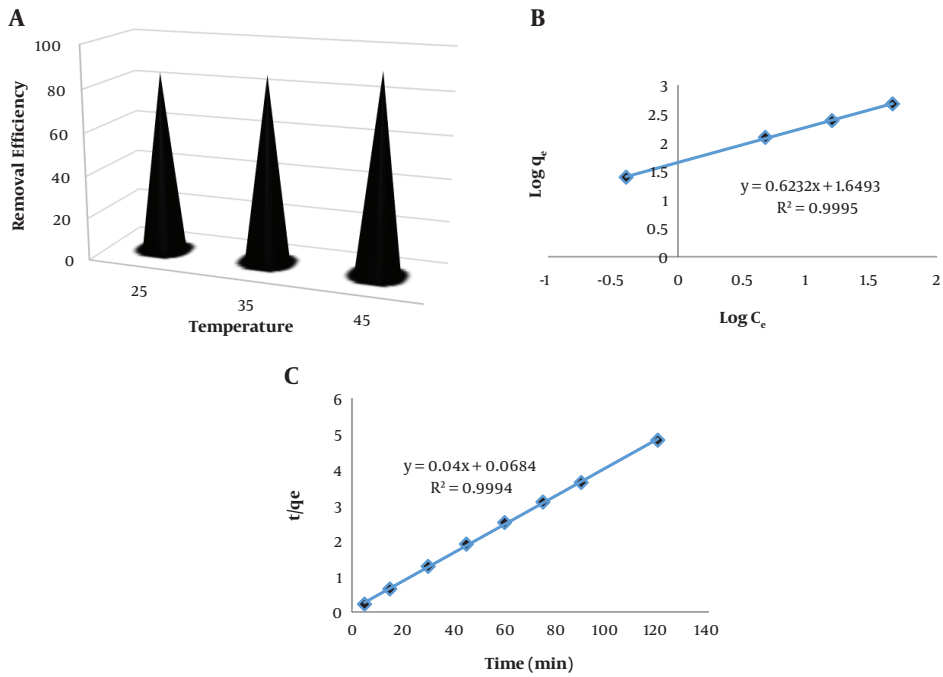

Figure 8. Effects of temperature (A), isotherm of Longmuir (B), and pseudo-second kinetic (C) adsorption of Malathion onto the SABM are represented

Table 1. Freundlich, Langmuir and Temkin Isotherm Parameters for the Adsorption of Malathion onto SABM Adsorbent

Langmuir Isotherm				Freundlich Isotherm			Temkin Isotherm		
R^2	K_a (L mg^{-1})	RL	q_m (mg g^{-1})	R^2	n	K_f	R^2	k_t (L mg^{-1})	b_1
0.852	17.24	0.011	36.76	0.9995	1.6	44.59	0.7636	6181	1.895

Table 2. Various Parameters of Kinetic Models for the Malathion Adsorption onto the SABM

q_e, experimental (mg/g)	Pseudo-First Order			Pseudo-Second Order			Intra-Particle Diffusion		
	R^2	k_1 (1/min)	q_e, calculated (mg/g)	R^2	k_2 (g/mg. min)	q_e, calculated (mg/g)	R^2	C (mg/g)	K_{id} (mg/g.$min^{1/2}$)
24.8	0.788	0.005	3	0.9813	0.023	25	0.85	9.65	0.22

the extent of adsorption (mg g^{-1}) and adsorption intensity of system calculated from plot of log q_e versus log C_e. Figure 7B shows Freundlich isotherm model for the adsorption of Malathion onto the SABM adsorbent, where coefficient of determination (R^2 = 0.9959) states that the adsorption process has good fit by Freundlich isotherm. Constants of Freundlich isotherm (K_f and n) prepared in Table 1 were 44.59 and 1.6, respectively. High amount of K_f constant represents very large extent of adsorption of Malathion onto the SABM adsorbent. Also, the value of n is larger than 1, indicating a favorable adsorption system and a multilayer physical process in the adsorption of Malathion by SABM adsorbent (35).

The Temkin model is employed to investigate the heat of the adsorption (adsorption energy) and adsorbent-adsorbate interactions. This isotherm assumes that the decrease of the adsorption energy of all the molecules in a layer linearly with the monolayer sorption on the active sites as a result of adsorbent-adsorbate interactions. The linear form of the Temkin model is given as follows (28, 36):

$$q_e = B_1 \, ln(K_t) + B_1 \, ln\,(C_e) \quad (6)$$

Where, B_1, $B_1 = RT/b_1$, denotes the Temkin constant (J/mol). R is the universal gas constant and equal to 8.314 J/mol.K. T is the absolute temperature (°K). k_t and b_1 represent the equilibrium binding constant (L/g) and adsorption heat (kJ/mol), respectively. Based on the data ob-

tained, the magnitude of b_1 value showed the fast removal of Malathion at the initial stage and the smallness of k_t value implied the weak bonding of Malathion molecules onto the composite.

4.8. Kinetic of Adsorption

To study the mechanism of Malathion adsorption onto the SABM adsorbent, the transient behavior of the Malathion adsorption process was investigated using the pseudo-first-order and pseudo-second-order kinetics which are explained as follows.

The pseudo-first-order kinetic. Linear equation of pseudo-first order kinetic is shown in Equation 6 (37).

$$Log\ (q_e - q_t) = Logq_e - \left(\frac{k_1}{2.303}\right) t \quad (7)$$

Where q_e, q_t, and k_1 refers to the amount of adsorbed Malathion at equilibrium (mg g^{-1}), the amount of adsorbed Malathion at time (t), and the equilibrium rate constant (min^{-1}) of pseudo-first-order kinetic, respectively. The k_1 is taken out from plotting *Log* (q_e - q_t) versus (t), where pseudo-first-order kinetic fitting for SABM adsorbent had a very poor coefficient of determination (R^2 = 0.7884) (not shown). Calculated pseudo-first-order kinetic constants were provided in Table 3. As shown in Table 3, the equilibrium adsorption capacity q_e (Cal) value was lower than the experimental q_e (Exp) value, which indicated the inapplicability of this model.

The pseudo-second-order equation. Linear form of pseudo-second-order kinetic is given in Equation 7 (27).

$$\frac{t}{q_t} = \frac{1}{k_2 q_e^2} + \frac{1}{q_e} t \quad (8)$$

By which, rate constant (k_2) and adsorption capacity in equilibrium (q_e) were calculated by plotting (t/q_t) versus (t) (Figure 7C). The initial adsorption rate (h) was calculated at zero time, by Equation 8.

$$h = k_2 q_e^2 \quad (9)$$

Additionally, the intraparticle diffusion model is conveniently employed to recognize the diffusion mechanism. The model can be epitomized as follows (38, 39):

$$q_t = k_{id}.t^{1/2} + C \quad (10)$$

Where, k_{id} (mg/g) is related to the intraparticle diffusion rate constant. C is the intercept and represents the thickness of the boundary layer (mg/g) in which the effect of this layer depends on the value of the intercept.

As shown in Figure 7C, the pseudo-second-order kinetic fitting for adsorption of Malathion onto the SABM adsorbent have a good coefficient of determination (R^2 = 0.9994). A similar behavior has been observed by Naushad et al. (31) on the removal of Malathion using amberlyst-15 resin. All the parameters of this kinetic model were prepared in Table 3. According to Table 3, the equilibrium adsorption capacity q_e (Cal) value (25 mg g^{-1}) was close to the experimental q_e *(Exp)* value (24.8 mg g^{-1}), which indicated the applicability of this kinetic model for the adsorption process behavior. Also, R_L is 14.37 (min^{-1} mg g^{-1}), which indicates the high initial adsorption rate. Based on the intraparticle diffusion model, the high values of C parameter (9.65) indicated that the boundary layer effect was also responsible for the adsorption. The multi-linearity of q versus $t^{0.5}$ plot, and/or deviation of the plots from the origin further confirms that the adsorption process is complex and some other mechanisms along with intraparticle diffusion control the process steps, as reported previously by Jerold et al. (40).

Table 3. Adsorption Capacities of Various Adsorbents for the Uptake of Malathion

Adsorbent	q_m (mg/g)	Refs.
Montmorillonite	7.95	(35)
Amberlyst-15 cation exchange resin	12.12	(31)
powdered activated carbon	21.74	(29)
De-Acidite FF-IP resin	16.39	(32)
SABM nanocomposite	36.86	This work

Abbreviation: SABM, sodium alginate/biosilicate/magnetite.

4.9. Thermodynamic Studies

The thermodynamic study was performed to reach a better understanding of the adsorptive behavior of Malathion toward nanocomposite. The free energy change (ΔG_0) (kJ mol^{-1}), enthalpy change (ΔH_0) (kJ mol^{-1}), and entropy change (ΔS_0) (kJ mol^{-1} K^{-1}) for the adsorption of Malathion were calculated by Equations 9 (26).

$$\Delta G = -RTlnKD \quad (11)$$

$$lnK_D = \left(\frac{\Delta S}{R}\right) - \left(\frac{\Delta H}{RT}\right) \quad (12)$$

The thermodynamic parameters of Malathion adsorption on MBAS are listed in Table 4. As represented in Table 4, the values of ΔH and ΔS are positive, and the standard free energy (ΔG) is negative. The positive ΔH value indicates that the sorption process was endothermic. In other words, the positivity of this parameter states that the increase in temperature has a positive effect on the adsorption of Malathion and, the adsorption of this pollutant at higher temperatures is more favorable. Furthermore, the negative values obtained for Gibbs free energy indicate that the adsorption of Malathion by the synthesized adsorbent is a spontaneous process (31).

Table 4. Thermodynamic Parameters for the Adsorption of Malathion on MBAS

Temperature (K)	Ln KD	ΔG_0 (kJ/mol)	ΔH_0 (kJ/mol)	ΔS_0 (kJ/mol.K)
298	1.81	-2.80	602.60	0.1
308	2.05	-4.05		
318	3.19	-5.78		

4.10. The Mechanisms of the Adsorption

The mechanism of the adsorption of organic pollutants onto inorganic materials usually are a combination of electrostatic interaction, ion exchange, π-π electron donor-acceptor (EDA) interaction, and hydrophobic surface interaction and so on.

The hydrophobic interaction is an important mechanism involved in the sorption of Malathion onto MBSA. Malathion is partially insoluble organics in water. As the pH increases, the Malathion molecules gain less water solubility and higher hydrophobicity; these results lead to a higher adsorption efficiency at pH 7. Therefore, the hydrophobic surface interactions should be a dominant mechanism in the adsorption process. In addition, electrostatic interaction can be a major mechanism governing adsorption of Malathion onto the MBSA (between the oppositely charged groups of adsorbate and adsorbent). Also, the acid-base interactions may be another significant factor involved in controlling Malathion adsorption.

4.11. Conclusions

To summarize, the characteristic analyses for the SABM adsorbent approved that the SABM adsorbent has high potential to adsorb the Malathion. Also, parameters, including pH, contact time, SABM dosage, Malathion concentration, and temperature influence the adsorption process. Owing to the high performance of this process at pH = 7, it expected the SABM adsorbent could be applicable to remove Malathion from real wastewater with natural pH value. Also, in determining isotherms of the Malathion adsorption, it was cleared the Freundlich isotherm model is better to describe this adsorption process, which is indicating multi-layer physical adsorption. Maximum monolayer adsorption capacity ($q_m = 36.76\ mg\ g^{-1}$) for SABM fungi particles can be illuminated by the SEM picture where there are numerous pores over the biosorbent surface. Moreover, the kinetic studies showed that the Malathion adsorption process followed the pseudo-second-order kinetic model. In general, the SABM adsorbent can be favorable for the removal of Malathion from aqueous solution.

Acknowledgments

The authors acknowledge Iran University of Medical Sciences for the financial support. We also acknowledge the School of Health for providing research facilities (project number; 32386).

Footnotes

Authors' Contribution: Mitra Gholami received the project. Mehdi Hosseini, Ali Esrafili, and MojtabaYegane Badi performed the experiments. Mehdi Hosseini, Hossein Kamani, and Ali Esrafili performed statistical analyses. Mehdi Hosseini and Mitra Gholami wrote the paper. All authors approved the final draft of the article.

Conflict of Interests: The authors declare no conflict of interest.

Funding/Support: The authors acknowledge Iran University of Medical Sciences for the financial support. We also acknowledge the School of Health for providing research facilities (project number: 32386).

References

1. Hela DG, Lambropoulou DA, Konstantinou IK, Albanis TA. Environmental monitoring and ecological risk assessment for pesticide contamination and effects in Lake Pamvotis, northwestern Greece. *Environ Toxicol Chem*. 2005;**24**(6):1548–56. doi: 10.1897/04-455r.1. [PubMed: 16117136].
2. Warren N, Allan IJ, Carter JE, House WA, Parker A. Pesticides and other micro-organic contaminants in freshwater sedimentary environments—a review. *Appl Geochem*. 2003;**18**(2):159–94. doi: 10.1016/s0883-2927(02)00159-2.
3. Dehghani R, Moosavi SG, Esalmi H, Mohammadi M, Jalali Z, Zamini N. Surveying of pesticides commonly on the markets of Iran in 2009. *J Environ Protect*. 2011;**2**(8):1113–7. doi: 10.4236/jep.2011.28129.
4. Ward MH, Nuckols JR, Weigel SJ, Maxwell SK, Cantor KP, Miller RS. Identifying populations potentially exposed to agricultural pesticides using remote sensing and a Geographic Information System. *Environ Health Perspect*. 2000;**108**(1):5–12. doi: 10.1289/ehp.001085. [PubMed: 10622770]. [PubMed Central: PMC1637858].
5. Al-Qurainy F, Abdel-Megeed A. Phytoremediation and detoxification of two organophosphorous pesticides residues in Riyadh area. *World Appl Sci J*. 2009;**6**(7):987–98.
6. World Health Organization. *Guidelines for drinking-water quality: Recommendations*. WHO; 2004.
7. Ohno K, Minami T, Matsui Y, Magara Y. Effects of chlorine on organophosphorus pesticides adsorbed on activated carbon: Desorption and oxon formation. *Water Res*. 2008;**42**(6-7):1753–9. doi: 10.1016/j.watres.2007.10.040. [PubMed: 18048077].
8. Ramos-Delgado NA, Hinojosa-Reyes L, Guzman-Mar IL, Gracia-Pinilla MA, Hernandez-Ramirez A. Synthesis by sol-gel of WO3/TiO2 for solar photocatalytic degradation of malathion pesticide. *Catalysis Today*. 2013;**209**:35–40. doi: 10.1016/j.cattod.2012.11.011.
9. Getzin LW, Rosefield I. Partial purification and properties of a soil enzyme that degrades the insecticide malathion. *Biochim Biophys Acta*. 1971;**235**(3):442–53. doi: 10.1016/0005-2744(71)90285-3. [PubMed: 5317645].
10. Doong RA, Chang WH. Photoassisted titanium dioxide mediated degradation of organophosphorus pesticides by hydrogen peroxide. *J Photochem Photobiol Chem*. 1997;**107**(1-3):239–44. doi: 10.1016/s1010-6030(96)04579-0.

11. Rani M, Shanker U. Effective adsorption and enhanced degradation of various pesticides from aqueous solution by Prussian blue nanorods. *J Environ Chem Eng*. 2018;**6**(1):1512–21. doi: 10.1016/j.jece.2018.01.060.
12. Younis SA, Ghobashy MM, Samy M. Development of aminated poly(glycidyl methacrylate) nanosorbent by green gamma radiation for phenol and malathion contaminated wastewater treatment. *J Environ Chem Eng*. 2017;**5**(3):2325–36. doi: 10.1016/j.jece.2017.04.024.
13. Liu Y, Chen M, Yongmei H. Study on the adsorption of Cu(II) by EDTA functionalized Fe3O4 magnetic nano-particles. *Chem Eng J*. 2013;**218**:46–54. doi: 10.1016/j.cej.2012.12.027.
14. Srivastava M, Singh J, Yashpal M, Gupta DK, Mishra RK, Tripathi S, et al. Synthesis of superparamagnetic bare Fe(3)O(4) nanostructures and core/shell (Fe(3)O(4)/alginate) nanocomposites. *Carbohydr Polym*. 2012;**89**(3):821–9. doi: 10.1016/j.carbpol.2012.04.016. [PubMed: 24750867].
15. Naghipour D, Taghavi K, Moslemzadeh M. Removal of methylene blue from aqueous solution by Artist's Bracket fungi: Kinetic and equilibrium studies. *Water Sci Technol*. 2016;**73**(11):2832–40. doi: 10.2166/wst.2016.147. [PubMed: 27232421].
16. Hossaini H, Moussavi G, Farrokhi M. The investigation of the LED-activated FeFNS-TiO2 nanocatalyst for photocatalytic degradation and mineralization of organophosphate pesticides in water. *Water Res*. 2014;**59**:130–44. doi: 10.1016/j.watres.2014.04.009. [PubMed: 24793111].
17. Darvishi Cheshmeh Soltani R, Safari M, Rezaee A, Godini H. Application of a compound containing silica for removing ammonium in aqueous media. *Environ Progr Sustain Energ*. 2015;**34**(1):105–11. doi: 10.1002/ep.11969.
18. Omidi Khaniabadi Y, Heydari R, Nourmoradi H, Basiri H, Basiri H. Low-cost sorbent for the removal of aniline and methyl orange from liquid-phase: Aloe Vera leaves wastes. *J Taiwan Inst Chem Eng*. 2016;**68**:90–8. doi: 10.1016/j.jtice.2016.09.025.
19. Darvishi Cheshmeh Soltani R, Safari M, Maleki A, Godini H, Mahmoudian MH, Pordel MA. Application of nanocrystalline Iranian diatomite in immobilized form for removal of a textile dye. *J Dispers Sci Tech*. 2015;**37**(5):723–32. doi: 10.1080/01932691.2015.1058715.
20. Mauter MS, Elimelech M. Environmental applications of carbon-based nanomaterials. *Environ Sci Technol*. 2008;**42**(16):5843–59. doi: 10.1021/es8006904. [PubMed: 18767635].
21. Zhao Y, Xue Z, Wang X, Wang L, Wang A. Adsorption of congo red onto lignocellulose/montmorillonite nanocomposite. *J Wuhan UnivTech Mater Sci Ed*. 2012;**27**(5):931–8. doi: 10.1007/s11595-012-0576-2.
22. Yi X, He J, Guo Y, Han Z, Yang M, Jin J, et al. Encapsulating Fe3O4 into calcium alginate coated chitosan hydrochloride hydrogel beads for removal of Cu (II) and U (VI) from aqueous solutions. *Ecotoxicol Environ Saf*. 2018;**147**:699–707. doi: 10.1016/j.ecoenv.2017.09.036. [PubMed: 28938140].
23. Darvishi Cheshmeh Soltani R, Safari M, Maleki A, Rezaee R, Shahmoradi B, Shahmohammadi S, et al. Decontamination of arsenic(V)-contained liquid phase utilizing Fe3O4/bone char nanocomposite encapsulated in chitosan biopolymer. *Environ Sci Pollut Res Int*. 2017;**24**(17):15157–66. doi: 10.1007/s11356-017-9128-9. [PubMed: 28500548].
24. Darvishi Cheshmeh Soltani R, Khataee AR, Godini H, Safari M, Ghanadzadeh MJ, Rajaei MS. Response surface methodological evaluation of the adsorption of textile dye onto biosilica/alginate nanobiocomposite: thermodynamic, kinetic, and isotherm studies. *Desalin Water Treat*. 2014;**56**(5):1389–402. doi: 10.1080/19443994.2014.950344.
25. Lou Z, Zhou Z, Zhang W, Zhang X, Hu X, Liu P, et al. Magnetized bentonite by Fe3O4 nanoparticles treated as adsorbent for methylene blue removal from aqueous solution: Synthesis, characterization, mechanism, kinetics and regeneration. *J Taiwan Inst Chem Eng*. 2015;**49**:199–205. doi: 10.1016/j.jtice.2014.11.007.
26. Darvishi Cheshmeh Soltani R, Khataee AR, Safari M, Joo SW. Preparation of bio-silica/chitosan nanocomposite for adsorption of a textile dye in aqueous solutions. *Int Biodeterior Biodegrad*. 2013;**85**:383–91. doi: 10.1016/j.ibiod.2013.09.004.
27. Pourkarim S, Ostovar F, Mahdavianpour M, Moslemzadeh M. Adsorption of chromium(VI) from aqueous solution by Artist's Bracket fungi. *Separ Sci Tech*. 2017;**52**(10):1733–41. doi: 10.1080/01496395.2017.1299179.
28. Massoudinejad M, Rasoulzadeh H, Ghaderpoori M. Magnetic chitosan nanocomposite: Fabrication, properties, and optimization for adsorptive removal of crystal violet from aqueous solutions. *Carbohydr Polym*. 2019;**206**:844–53. doi: 10.1016/j.carbpol.2018.11.048. [PubMed: 30553392].
29. Kumar P, Singh H, Kapur M, Mondal MK. Comparative study of malathion removal from aqueous solution by agricultural and commercial adsorbents. *J Water Proc Eng*. 2014;**3**:67–73. doi: 10.1016/j.jwpe.2014.05.010.
30. Zhang Q, Jing Y, Shiue A, Chang CT, Ouyang T, Lin CF, et al. Photocatalytic degradation of malathion by TiO(2) and Pt-TiO(2) nanotube photocatalyst and kinetic study. *J Environ Sci Health B*. 2013;**48**(8):686–92. doi: 10.1080/03601234.2013.778623. [PubMed: 23638896].
31. Naushad M, Alothman ZA, Khan MR, Alqahtani NJ, Alsohaimi IH. Equilibrium, kinetics and thermodynamic studies for the removal of organophosphorus pesticide using Amberlyst-15 resin: Quantitative analysis by liquid chromatography–mass spectrometry. *J Ind Eng Chem*. 2014;**20**(6):4393–400. doi: 10.1016/j.jiec.2014.02.006.
32. Naushad M, Alothman ZA, Khan MR. Removal of malathion from aqueous solution using De-Acidite FF-IP resin and determination by UPLC-MS/MS: equilibrium, kinetics and thermodynamics studies. *Talanta*. 2013;**115**:15–23. doi: 10.1016/j.talanta.2013.04.015. [PubMed: 24054556].
33. Balarak D, Mahdavi Y, Bazrafshan E, Mahvi AH, Esfandyari Y. Adsorption of fluoride from aqueous solutions by carbon nanotubes: Determination of equilibrium, kinetic, and thermodynamic parameters. *Adsorption*. 2016;**49**(1):71–83.
34. Bazrafshan E, Zarei AA, Nadi H, Zazouli MA. Adsorptive removal of Methyl Orange and Reactive Red 198 dyes by Moringa peregrina ash. *Indian J Chem Tech (IJCT)*. 2014;**21**(2):105–13.
35. Pal OR, Vanjara AK. Removal of malathion and butachlor from aqueous solution by clays and organoclays. *Separ Purif Tech*. 2001;**24**(1-2):167–72. doi: 10.1016/s1383-5866(00)00226-4.
36. Bazrafshan E, Kord Mostafapour F, Rahdar S, Mahvi AH. Equilibrium and thermodynamics studies for decolorization of Reactive Black 5 (RB5) by adsorption onto MWCNTs. *Desalin Water Treat*. 2014;**54**(8):2241–51. doi: 10.1080/19443994.2014.895778.
37. Zhao J, Liu J, Li N, Wang W, Nan J, Zhao Z, et al. Highly efficient removal of bivalent heavy metals from aqueous systems by magnetic porous Fe3O4 -MnO2: Adsorption behavior and process study. *Chem Eng J*. 2016;**304**:737–46. doi: 10.1016/j.cej.2016.07.003.
38. Alimohammadi M, Saeedi Z, Akbarpour B, Rasoulzadeh H, Yetilmezsoy K, Al-Ghouti MA, et al. Adsorptive removal of arsenic and mercury from aqueous solutions by Eucalyptus leaves. *Water Air Soil Pollut*. 2017;**228**(11). doi: 10.1007/s11270-017-3607-y.
39. Balarak D, Kord Mostafapour F, Bazrafshan E, Mahvi AH. The equilibrium, kinetic, and thermodynamic parameters of the adsorption of the fluoride ion on to synthetic nano sodalite zeolite. *Fluoride*. 2017;**50**(2):223–34.
40. Jerold M, Vasantharaj K, Joseph D, Sivasubramanian V. Fabrication of hybrid biosorbent nanoscale zero-valent iron-Sargassum swartzii biocomposite for the removal of crystal violet from aqueous solution. *Int J Phytoremediation*. 2017;**19**(3):214–24. doi: 10.1080/15226514.2016.1207607. [PubMed: 27420340].